Nonlinear Dynamics (2005) 42: 199–215

Three-Dimensional Large Deformation Analysis of the Multibody Pantograph/Catenary Systems

JONG-HWI SEO[1], HIROYUKI SUGIYAMA[2], and AHMED A. SHABANA[2,*]

[1]*Department of Mechanical Engineering, Ajou University, Suwon, Gyeounggi-Do, 443-749, Korea;* [2]*Department of Mechanical and Industrial Engineering, University of Illinois at Chicago, 842 West Taylor Street, Chicago, IL 60607-7022, U.S.A.;* *Author for correspondence (e-mail: shabana@uic.edu; fax: +1-312-413-0447)*

(Received: 10 December 2004; accepted: 15 February 2005)

Abstract. To accurately model the nonlinear behavior of the pantograph/catenary systems, it is necessary to take into consideration the effect of the large deformation of the catenary and its interaction with the nonlinear pantograph system dynamics. The large deformation of the catenary is modeled in this investigation using the three-dimensional finite element absolute nodal coordinate formulation. To model the interaction between the pantograph and the catenary, a sliding joint that allows for the motion of the pan-head on the catenary cable is formulated. To this end, a non-generalized arc-length parameter is introduced in order to be able to accurately predict the location of the point of contact between the pan-head and the catenary. The resulting system of differential and algebraic equations formulated in terms of reference coordinates, finite element absolute nodal coordinates, and non-generalized arc-length and contact surface parameters are solved using computational multibody system algorithms. A detailed three-dimensional multibody railroad vehicle model is developed to demonstrate the use of the formulation presented in this paper. In this model, the interaction between the wheel and the rail is considered. For future research, a method is proposed to deal with the problem of the loss of contact between the pan-head and the catenary cable.

Key words: multibody dynamics, pantograph/catenary interactions, railroad vehicles, sliding joints

1. Introduction

In the analysis of the pantograph/catenary interactions in railroad vehicle systems, accurate predictions of the contact forces are crucial to accurately determine the stability and dynamic characteristics of the system and to evaluate the effect of the loss of contact and wear of catenary cables. Despite the fact that general multibody algorithms that are based on accurate wheel/rail contact formulations [1–8] have been successfully used in the nonlinear dynamic analysis of railroad vehicle systems, the use of these algorithms in the dynamic analysis of the pantograph/catenary systems have been very limited. The limited use and success of existing multibody system approaches in the analysis of the pantograph/catenary systems can be attributed to two main reasons. The first is due to the fact that most general-purpose multibody computer programs employ the floating frame of reference formulation which was developed to solve small deformation problems, and therefore, these programs cannot be used to systematically and efficiently solve the pantograph/catenary problem because of the catenary large deformation. The second reason for the limited use of multibody system algorithms in the analysis of the pantograph/catenary system is the lack of an accurate formulation for a sliding joint in which one body slides on another very flexible body. This is a problem of moving boundary conditions that cannot be efficiently formulated in computational multibody system algorithms using approaches that are based on linear or component modes.

It is, therefore, the objective of this investigation to address these two difficulties by adopting a large deformation finite element formulation that can be systematically used to develop the sliding

joints between two components; one of them can be very flexible. In existing approaches used for the dynamic analysis of the pantograph/catenary interactions, three different methods are often used to model the deformation of the catenary cables. In the first method, springs are used to model the dynamic interactions between the catenary and the pantograph [9–11]. While this simple method provides an insight into the dynamics and stability of the pantograph/catenary system, this approach is too simple to accurately account for the effect of the nonlinear deformation of the cable and the high frequency vibrations arising from the pantograph/catenary interactions. Furthermore, there is no general procedure that can be used to determine the lumped parameters of the model. In the second approach, the catenary is modeled as a continuous string or beam using partial differential equations [12–14]. While the partial differential equations can be used to study the wave propagations in the catenary cables, the use of this approach is not suited for implementation in computational multibody computer algorithms [12]. In the third approach, the catenary cables are modeled using a linear finite element formulation [15]. In these models, the moving contact load acting on the catenary is applied as an external force [9, 15]. Such models, therefore, do not account for many of the coupling effects and nonlinearities due to the pantograph/catenary contact.

As previously pointed out, accurate modeling of the contact between the flexible catenary cable and the pantograph is one of the challenging problems since the locations of the contact point on the catenary cable is time and space dependant. Modeling this contact requires the use and computer implementation of the non-incremental large deformation finite element absolute nodal coordinate formulation [16–19]. In addition to the absolute position and gradient nodal coordinates used in this formulation, an arc-length parameter needs to be introduced to determine the exact location of the contact point on line. This arc-length parameter enters in the formulation of the sliding joint between the pan-head and the very flexible catenary cable [16, 20]. Two other sets of coordinates need to be introduced to be able to analyze a detailed railroad vehicle model including the pantograph/catenary system. A set of reference-generalized coordinates is used in the multibody system formulations to define the system configuration, and a second set of non-generalized surface parameters is used to describe the wheel/rail contact conditions. Therefore, in this investigation, the kinematic and dynamic equations of the multibody railroad vehicle model that includes the pantograph/catenary system are formulated using four different sets of coordinates; reference coordinates that describe the rigid body motion of the system components, absolute nodal coordinates that describe the large deformation of the catenary system, non-generalized surface parameters that define the wheel and rail profile geometry and non-generalized arc-length parameters that enter in the formulation of the sliding joint between the pan-head and the catenary system. These coupled sets of coordinates are used in this study to formulate the nonlinear dynamic equations of railroad vehicle systems that include the pantograph/catenary mechanism. The use of the formulation introduced in this paper is demonstrated using a detailed three-dimensional railroad vehicle model. It is important to point out that in the finite element absolute nodal coordinate formulation used in this investigation to model the large deformation of the catenary cable, there is no restriction on the amount of rotation or deformation within the element and as a result a non-incremental solution procedure that is suited for the use in multibody system computational algorithms can be adopted. In Section 8, it will be explained how the sliding joint formulation presented in this section can be modified in order to account for the loss of contact, a problem that will be the subject of future investigations.

2. Generalized and Non-Generalized Coordinates

Detailed multibody vehicle models can consist of a large number of components connected by joints and force elements such as springs, dampers and friction elements. Some of these components can be

modeled as rigid bodies; some as flexible bodies; and the others, such as the catenary cables, as very flexible bodies. Efficient computer implementation of an algorithm that is used to solve railroad vehicle problems requires the use of different sets of generalized coordinates to model bodies with different degrees of flexibility. For rigid bodies, a set of reference coordinate $\mathbf{q}_r^i$ is used to describe the location of the origin and the orientation of the selected body coordinate system. For flexible bodies two sets of coordinates are used; $\mathbf{q}_r^i$ and $\mathbf{q}_f^i$, where the vector $\mathbf{q}_r^i$ describes the motion of the flexible body coordinate system, and the vector $\mathbf{q}_f^i$ describes the small deformation of the body with respect to its coordinate system [18]. Using the floating frame of reference formulation, the location of an arbitrary point on the flexible body can be written as:

$$\mathbf{r}^i = \mathbf{R}^i + \mathbf{A}^i \bar{\mathbf{u}}^i \tag{1}$$

where $\mathbf{R}^i$ is the vector that defines the location of the origin of the body coordinate system, $\mathbf{A}^i$ is the transformation matrix that defines the orientation of the body coordinate system, and $\bar{\mathbf{u}}^i$ is the local position vector of the arbitrary point with respect to the body coordinate system. In the case of rigid bodies, the vector $\bar{\mathbf{u}}^i$ is constant, whereas in the case of flexible bodies $\bar{\mathbf{u}}^i$ depends on the vector of elastic coordinates $\mathbf{q}_f^i$. The transformation matrix $\mathbf{A}^i$ can be defined in terms of a selected set of orientation parameters $\boldsymbol{\theta}^i$. In this case, the vector of reference coordinates is defined as $\mathbf{q}_r^i = [\mathbf{R}^{i^{\mathrm{T}}}\ \boldsymbol{\theta}^{i^{\mathrm{T}}}]^{\mathrm{T}}$.

In the case of very flexible bodies, such as the catenary cables, the configuration of the body is described using the absolute nodal coordinate formulation [19]. In this formulation, the vector of absolute nodal coordinates $\mathbf{e}^i$ is used. In the absolute nodal coordinate formulation, the global position vector of an arbitrary point on element e of beam i as shown in Figure 1 can be defined in a global coordinate system XYZ as

$$\mathbf{r}^{ie} = \mathbf{S}^{ie}(x^{ie}, y^{ie}, z^{ie})\ \mathbf{e}^{ie} \tag{2}$$

where $\mathbf{S}^{ie}(x^{ie}, y^{ie}, z^{ie})$ is the element shape function matrix, x^{ie}, y^{ie} and z^{ie} are the spatial coordinates defined in the element coordinate system, and $\mathbf{e}^{ie}$ is the vector of nodal coordinates of element e on beam i. The element shape function matrix and the element nodal coordinates used in this investigation

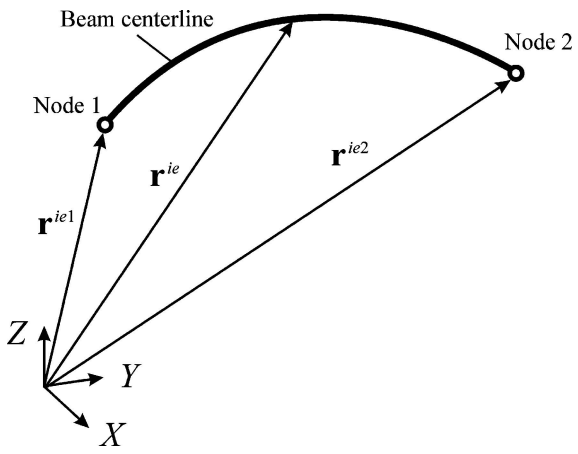

Figure 1. Absolute nodal coordinates.

for a three-dimensional beam element are presented in the literature [19]. The nodal coordinate vector $\mathbf{e}^{iek}$ at node k can be defined using 12 nodal coordinates as follows:

$$\mathbf{e}^{iek} = \left[(\mathbf{r}^{iek})^{\mathrm{T}} \quad \left(\frac{\partial \mathbf{r}^{iek}}{\partial x^{ie}}\right)^{\mathrm{T}} \quad \left(\frac{\partial \mathbf{r}^{iek}}{\partial y^{ie}}\right)^{\mathrm{T}} \quad \left(\frac{\partial \mathbf{r}^{iek}}{\partial z^{ie}}\right)^{\mathrm{T}} \right]^{\mathrm{T}} \tag{3}$$

where $\mathbf{r}^{iek}$ is the global position vector at node k and $\partial \mathbf{r}^{iek}/\partial x^{ie}$, $\partial \mathbf{r}^{iek}/\partial y^{ie}$ and $\partial \mathbf{r}^{iek}/\partial z^{ie}$ define the gradients of the global position vector at node k. This representation ensures inter-element continuity of the global displacement gradients at the nodal points without making any assumptions regarding the magnitude of the rotation or deformation within the element [19].

The configuration of the multibody railroad vehicle system can, therefore, be described using the generalized coordinates $\mathbf{q}_r$, $\mathbf{q}_f$ and $\mathbf{e}$ which describe, respectively, the reference motion, the small deformation, and the large deformation. In addition to these generalized coordinates, surface and arc-length parameters $\mathbf{s}$ need to be introduced to describe the wheel/rail contact [2, 5–7] and the pantograph/catenary contact. Therefore, the vector of system generalized and non-generalized coordinates can be written as

$$\mathbf{q} = \left[\mathbf{q}_r^{\mathrm{T}} \quad \mathbf{q}_f^{\mathrm{T}} \quad \mathbf{e}^{\mathrm{T}} \quad \mathbf{s}^{\mathrm{T}} \right]^{\mathrm{T}} \tag{4}$$

The components of this vector will be used in the following sections to formulate the kinematic and dynamic equations of multibody railroad vehicle systems.

3. Kinematics of Pantograph/Catenary Contact

The contact between the pantograph and catenary requires a formulation that involves a very flexible body. In this section, the formulation of the sliding joint between the pan-head and the very flexible catenary is discussed. In Section 8, it is explained how the sliding joint formulation presented in this section can be modified to account for the loss of contact between the pan-head and the catenary cable. The sliding joint used in this study allows relative motion of two bodies; one body moves along a deformable joint axis defined on the other flexible body, as shown in Figure 2. The constraints of a simple sliding joint defined at contact point P can be written as follows [16]:

$$\mathbf{C}^{ij}(\mathbf{e}^{ie}, \mathbf{q}^{j}, s^{ie}) = \mathbf{r}_P^{ie} - \mathbf{r}_P^{j} = \mathbf{0} \tag{5}$$

where body i is assumed to be a very flexible body that can represent the catenary cable modeled using the absolute nodal coordinate formulation, and body j is assumed to be a rigid, flexible or very flexible body defined by the generalized coordinates $\mathbf{q}^j = [\mathbf{q}_r^{j^{\mathrm{T}}} \ \mathbf{q}_f^{j^{\mathrm{T}}}]^{\mathrm{T}}$ or $\mathbf{e}^j$. The location of the contact point can be defined using the arc-length parameter s^{ie} defined on element e of body i as shown in Figure 2. In the preceding equation, $\mathbf{r}_P^{ie}$ and $\mathbf{r}_P^{j}$ are, respectively, the global position vectors of the contact point on the catenary cable and the pan-head. If body j slides on the cable centerline, the global position vector of point P of body i can be defined as

$$\mathbf{r}_P^{ie} = \mathbf{S}^{ie}(s^{ie}, 0, 0)\,\mathbf{e}^{ie} \tag{6}$$

It is important to point out that if the cable is straight in the undeformed configuration, $s^{ie} = x^{ie}$ which is the assumption made in this investigation. Note that Equation (5) has three scalar constraint

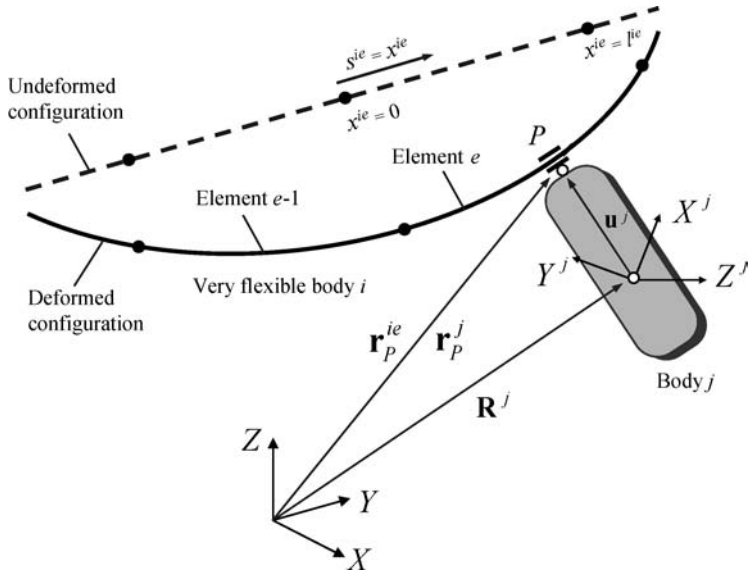

Figure 2. Sliding joint on the flexible cable.

equations that can be used to eliminate two degrees of freedom since the arc-length parameter s^{ie} is also an unknown variable. Consequently, Equation (5) leads to only two independent constraint forces that prevent the relative motion between the two bodies in a plane perpendicular to the cable centerline. The sliding joint constraint equations of Equation (5) can also be written in the following form:

$$\mathbf{C}^{ij}(\mathbf{e}^{ie}, \mathbf{q}^j, s^{ie}) = \begin{bmatrix} \mathbf{i}_t^{ie} \cdot \mathbf{r}_P^{ij} \\ \mathbf{j}_t^{ie} \cdot \mathbf{r}_P^{ij} \\ \mathbf{k}_t^{ie} \cdot \mathbf{r}_P^{ij} \end{bmatrix} \tag{7}$$

where $\mathbf{r}_P^{ij} = \mathbf{r}_P^{ie} - \mathbf{r}_P^j$ and $\mathbf{i}_t^{ie}$, $\mathbf{j}_t^{ie}$ and $\mathbf{k}_t^{ie}$ are unit vectors that define a *tangent frame* [16] whose $\mathbf{i}_t^{ie}$ axis is tangent to the space curve of the catenary cable. The transformation matrix that defines the orientation of the tangent frame is given by [16].

$$\mathbf{A}_t^{ie}(\mathbf{e}^{ie}, s^{ie}) = \begin{bmatrix} \mathbf{i}_t^{ie} & \mathbf{j}_t^{ie} & \mathbf{k}_t^{ie} \end{bmatrix} \tag{8}$$

where the orthogonal unit vectors $\mathbf{i}_t^{ie}$, $\mathbf{j}_t^{ie}$ and $\mathbf{k}_t^{ie}$ are defined using the following equations:

$$\mathbf{i}_t^{ie} = \frac{\mathbf{r}_s^{ie}}{\left|\mathbf{r}_s^{ie}\right|} = \hat{\mathbf{r}}_s^{ie}, \quad \mathbf{k}_t^{ie} = \frac{\mathbf{i}_t^{ie} \times \mathbf{r}_y^{ie}}{\left|\mathbf{i}_t^{ie} \times \mathbf{r}_y^{ie}\right|}, \quad \mathbf{j}_t^{ie} = \mathbf{k}_t^{ie} \times \mathbf{i}_t^{ie} \tag{9}$$

where $\mathbf{r}_s^{ie} = \partial \mathbf{r}_P^{ie} / \partial s^{ie}$, and $\mathbf{r}_y^{ie} = \partial \mathbf{r}_P^{ie} / \partial y^{ie}$. Here $\mathbf{r}_s^{ie}$ is not, in general, a unit vector since $s^{ie} = x^{ie}$ is assumed to be the arc length in the undeformed straight configuration. The sliding joint constraints of Equation (7) must be imposed at the position, velocity and acceleration levels. To this end, these constraints must be differentiated twice with respect to time. To illustrate the procedure for obtaining

these derivatives, we consider the first time derivative of the first constraint in Equation (7). This derivative is defined as follows:

$$\dot{C}_1^{ij} = \dot{\mathbf{i}}_t^{ie} \cdot \dot{\mathbf{r}}_P^{ij} + \mathbf{r}_P^{ij} \cdot \dot{\mathbf{i}}_t^{ie} = \mathbf{C}_{1\mathbf{q}}^{ij} \dot{\mathbf{q}}^{ij} + C_{1s}^{ij} \dot{s}^{ie} \tag{10}$$

where $\mathbf{q}^{ij} = [\mathbf{e}^{ie^{\mathrm{T}}}\ \mathbf{q}^{j^{\mathrm{T}}}]^{\mathrm{T}}$ and

$$\mathbf{C}_{1\mathbf{q}}^{ij} = \mathbf{i}_t^{ie^{\mathrm{T}}} \frac{\partial \mathbf{r}_P^{ij}}{\partial \mathbf{q}^{ij}} + \mathbf{r}_P^{ij^{\mathrm{T}}} \frac{\partial \mathbf{i}_t^{ie}}{\partial \mathbf{q}^{ij}}, \quad \mathbf{C}_{1s}^{ij} = \mathbf{i}_t^{ie^{\mathrm{T}}} \frac{\partial \mathbf{r}_P^{ij}}{\partial s^{ie}} + \mathbf{r}_P^{ij^{\mathrm{T}}} \frac{\partial \mathbf{i}_t^{ie}}{\partial s^{ie}} \tag{11}$$

Using the definition given in Equation (9), the derivative of the vector $\mathbf{i}_t^{ie}$ with respect to the generalized coordinates $\mathbf{q}^{ij}$ and the non-generalized arc-length parameter s^{ie} can be obtained as

$$\frac{\partial \mathbf{i}_t^{ie}}{\partial \mathbf{q}^{ij}} = \frac{\partial \hat{\mathbf{r}}_s^{ie}}{\partial \mathbf{r}_s^{ie}} \frac{\partial \mathbf{r}_s^{ie}}{\partial \mathbf{q}^{ij}}, \quad \frac{\partial \mathbf{i}_t^{ie}}{\partial s^{ie}} = \frac{\partial \hat{\mathbf{r}}_s^{ie}}{\partial \mathbf{r}_s^{ie}} \frac{\partial \mathbf{r}_s^{ie}}{\partial s^{ie}} \tag{12}$$

Since $\mathbf{r}_s^{ie} = \mathbf{S}^{ie'}\mathbf{e}^{ie}$, one has $\partial \mathbf{r}_s^{ie}/\partial \mathbf{e}^{ie} = \mathbf{S}^{ie'}$ and $\partial \mathbf{r}_s^{ie}/\partial s^{ie} = \mathbf{S}^{ie''}\mathbf{e}^{ie}$, where $\mathbf{a}'$ denotes the differentiation of $\mathbf{a}$ with respect to s. Note that

$$\frac{\partial \mathbf{r}_P^{ij}}{\partial \mathbf{q}^{ij}} = \begin{bmatrix} \dfrac{\partial \mathbf{r}_P^{ie}}{\partial \mathbf{e}^{ie}} & \dfrac{\partial \mathbf{r}_P^{j}}{\partial \mathbf{q}^{j}} \end{bmatrix}, \quad \frac{\partial \mathbf{r}_P^{ij}}{\partial s^{ie}} = \frac{\partial \mathbf{r}_P^{ie}}{\partial s^{ie}} \tag{13}$$

where $\partial \mathbf{r}_P^{ie}/\partial s^{ie} = \mathbf{S}^{ie'}\mathbf{e}^{ie}$.

Differentiating Equation (10) once more with respect to time, one obtains

$$\ddot{C}_1^{ij} = \mathbf{i}_t^{ie} \cdot \ddot{\mathbf{r}}_P^{ij} + \mathbf{r}_P^{ij} \cdot \ddot{\mathbf{i}}_t^{ie} + 2\dot{\mathbf{i}}_t^{ie} \cdot \dot{\mathbf{r}}_P^{ij} = \mathbf{C}_{1\mathbf{q}}^{ij} \ddot{\mathbf{q}}^{ij} + C_{1s}^{ij} \ddot{s}^{ie} + Q_d^{ij} = 0 \tag{14}$$

where Q_d^{ij} includes all the quadratic velocity terms that result from the second differentiation of the constraint with respect to time. A similar procedure can be used to obtain the first and second derivatives of the second and third constraints of Equation (7). In Section 5, two methods will be discussed to impose the sliding joint constraints at the position, velocity and acceleration levels. In the first method, the non-generalized arc-length parameter is not eliminated from the final form of the equations of motion, while in the second method this parameter is systematically eliminated using an embedding technique.

4. Wheel/Rail Contact

The wheel/rail contact forces have a significant effect on the railroad vehicle stability [1–7]. These forces depend on the location of the contact points, material properties of the wheel and rail, vehicle speed, and the geometric properties of the contact surfaces. The geometry of the surfaces of the wheel and rail are described using surface parameters that can be used to determine the location of the contact points. In the constraint formulations, the contact between two surfaces can be described using a set of nonlinear algebraic equations that must be imposed at the position, velocity, and acceleration levels. One may choose not to eliminate the surface parameters, leading to an augmented form of the equations of motion expressed in terms of the Lagrange multipliers associated with the kinematic contact constraint equations. Alternatively, one may choose to systematically eliminate the surface parameters using the

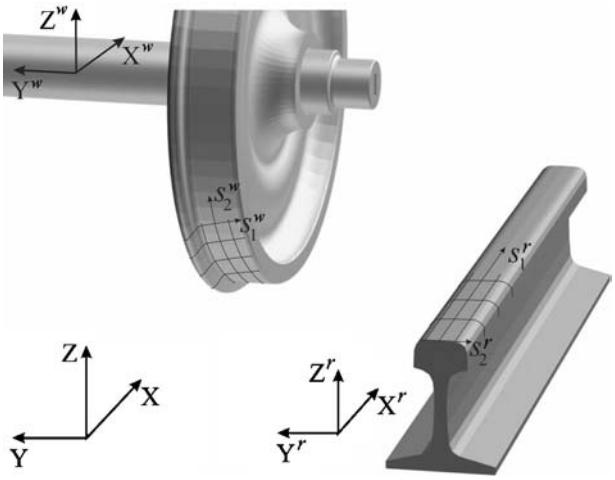

Figure 3. Surface parameters of the wheel and rail.

contact constraints, leading to an embedding formulation of the equations of motion that does not explicitly include the surface parameter accelerations.

4.1. Track and Wheel Geometries

To determine the location of the point of contact between two bodies, a complete parameterization of the surfaces must be used [2]. In general, a set of four surface parameters is used to describe the geometry of the two surfaces in contact as shown in Figure 3. The surface parameters can be written in a vector form as

$$\mathbf{s} = \begin{bmatrix} s_1^w & s_2^w & s_1^r & s_2^r \end{bmatrix}^{\mathrm{T}} \tag{15}$$

where superscripts r and w denote wheel and rail, respectively. Using these parameters, the location of the contact point P can be defined in the body coordinate systems as

$$\bar{\mathbf{u}}_P^w\left(s_1^w, s_2^w\right) = \begin{bmatrix} \bar{x}^w\left(s_1^w, s_2^w\right) \\ \bar{y}^w\left(s_1^w, s_2^w\right) \\ \bar{z}^w\left(s_1^w, s_2^w\right) \end{bmatrix}, \quad \bar{\mathbf{u}}_P^r\left(s_1^r, s_2^r\right) = \begin{bmatrix} \bar{x}^r\left(s_1^r, s_2^r\right) \\ \bar{y}^r\left(s_1^r, s_2^r\right) \\ \bar{z}^r\left(s_1^r, s_2^r\right) \end{bmatrix} \tag{16}$$

The tangents to the rail surface at the contact point are defined in the body coordinate system as

$$\bar{\mathbf{t}}_1^r = \frac{\partial \bar{\mathbf{u}}_P^r}{\partial s_1^r}, \quad \bar{\mathbf{t}}_2^r = \frac{\partial \bar{\mathbf{u}}_P^r}{\partial s_2^r} \tag{17}$$

and the normal vector as

$$\bar{\mathbf{n}}^r = \bar{\mathbf{t}}_1^r \times \bar{\mathbf{t}}_2^r \tag{18}$$

The surface parameters s_1^r and s_2^r are defined in a rail profile coordinate system. The location of the origin and the orientation of the profile coordinate system, defined respectively by the vector $\mathbf{R}^{rp}$ and

the transformation matrix $\mathbf{A}^{rp}$, can be uniquely determined using the surface parameter s_1^r [5]. Using this description, the global position vector of an arbitrary point on the surface of the rail r can be written as follows [5]:

$$\mathbf{r}^r = \mathbf{R}^r + \mathbf{A}^r(\mathbf{R}^{rp} + \mathbf{A}^{rp}\bar{\mathbf{u}}^{rp}) \tag{19}$$

where $\mathbf{R}^r$ is the global position vector of the origin of the rail coordinate system, $\mathbf{A}^r$ is the transformation matrix that defines the orientation of the rail coordinate system, and $\bar{\mathbf{u}}^{rp}$ is the local position vector that defines the location of the arbitrary point on the rail surface with respect to the profile coordinate system.

Similarly, the geometry of the wheel surface can be described using the two surface parameters s_1^w and s_2^w shown in Figure 3. The location of the origin and the orientation of the wheel set coordinate system are defined, respectively, by the vector $\mathbf{R}^w$ and the transformation matrix $\mathbf{A}^w$. Using this description, the global position vector of an arbitrary point on the surface of the wheel w can be written as follows [5]:

$$\mathbf{r}^w = \mathbf{R}^w + \mathbf{A}^w\bar{\mathbf{u}}^w \tag{20}$$

where $\bar{\mathbf{u}}^w$ is the local position vector that defines the location of the arbitrary point on the wheel surface with respect to the wheel set coordinate system.

4.2. Wheel/Rail Contact Constraints

There are, in general, two different approaches used to solve the wheel/rail contact problems. The first approach is the *contact constraint* approach in which the contact between the wheel and rail surfaces is described using nonlinear algebraic kinematic constraint equations [1, 2]. These equations can be solved along with the equations of motion using the technique of Lagrange multipliers and the augmented form of the dynamic equations. The normal contact forces are determined in this formulation as constraint forces associated with the contact constraints. The second approach used is the *elastic contact* formulation [3–6]. In this formulation, the normal contact forces are modeled using compliant forces based on the Hertzian contact theory or using an assumed compliant force model. Small local deformations in the contact area are used to define the normal contact force. In this investigation, the constraint contact formulation is used. Comparison between the two different contact formulations can be found in the literature [7].

When the wheel and rail come into contact, two sets of non-conformal kinematic contact conditions need to be satisfied [2]. First, two points (contact points) on the two surfaces coincide; and second, the two surfaces must have the same tangent plane at the contact point. These two conditions define the following five constraint equations that are required to describe the non-conformal contact between the wheel and rail:

$$\mathbf{C}^k(\mathbf{q}^w, \mathbf{q}^r, \mathbf{s}^{wk}, \mathbf{s}^{rk}) = \begin{bmatrix} \mathbf{r}_P^w - \mathbf{r}_P^r \\ \mathbf{t}_1^w \cdot \mathbf{n}^r \\ \mathbf{t}_2^w \cdot \mathbf{n}^r \end{bmatrix}^k = \mathbf{0} \tag{21}$$

or equivalently [7],

$$\mathbf{C}^k(\mathbf{q}^w, \mathbf{q}^r, \mathbf{s}^{wk}, \mathbf{s}^{rk}) = \begin{bmatrix} \mathbf{t}_1^r \cdot \left(\mathbf{r}_P^w - \mathbf{r}_P^r\right) \\ \mathbf{t}_2^r \cdot \left(\mathbf{r}_P^w - \mathbf{r}_P^r\right) \\ \mathbf{n}^r \cdot \left(\mathbf{r}_P^w - \mathbf{r}_P^r\right) \\ \mathbf{t}_1^w \cdot \mathbf{n}^r \\ \mathbf{t}_2^w \cdot \mathbf{n}^r \end{bmatrix}^k = \mathbf{0} \tag{22}$$

where superscript k denotes the contact number, superscript r and w denote rail and wheel, respectively, $\mathbf{q}^w$ and $\mathbf{q}^r$ are, respectively, the generalized coordinates of wheel and rail, and $\mathbf{t}_1$, $\mathbf{t}_2$ and $\mathbf{n}$ are the two tangents and normal to the surface at the contact point. In Equation (22), the three relative displacement constraints (point constraints) are defined in a rail coordinate system at the contact point. The first three point constraints of Equation (21), on the other hand, are defined in the global coordinate system. Note that the preceding contact constraint equations, as in the case of the pantograph/catenary contact, are expressed in terms of the generalized coordinates and non-generalized surface parameters.

5. Multibody Equations of Motion

The pantograph/catenary and wheel/rail contact constraints, as shown in the preceding two sections, are expressed in terms of the system component generalized coordinates as well as the non-generalized surface parameters that must be introduced to accurately determine the location of the contact points. As previously pointed out, the generalized coordinates include reference and elastic coordinates used in the floating frame of reference formulation to solve rigid body and small deformation problems [18] as well as absolute nodal coordinates used in the absolute nodal coordinate formulation to solve the large deformation problem encountered when modeling the pantograph/catenary system. In this section, the equations of motion used in this investigation to study the dynamics of railroad vehicle models that include the pantograph/catenary system are discussed.

It can be shown that the use of the fact that the mass matrix associated with absolute nodal coordinates $\mathbf{e}$ is constant, one can construct a constant transformation and use it to write $\mathbf{e}$ in term of a new set of coordinates, called the *Cholesky coordinates* $\mathbf{q}_{ch}$. The use of the Cholesky coordinates $\mathbf{q}_{ch}$ leads to an identity mass matrix associated with the Cholesky coordinates [21]. Using this transformation, the vector of system generalized and non-generalized coordinates can be written as

$$\mathbf{q} = \begin{bmatrix} \mathbf{q}_r^{\mathrm{T}} & \mathbf{q}_f^{\mathrm{T}} & \mathbf{q}_{ch}^{\mathrm{T}} & \mathbf{s}^{\mathrm{T}} \end{bmatrix}^{\mathrm{T}} \tag{23}$$

In this vector, the non-generalized coordinate vector $\mathbf{s}$ consists of the arc-length parameters used in the formulation of the pantograph/catenary sliding joints and the surface parameters used in the formulation of the wheel/rail contact constraints. The joint, driving and contact constraints (see Equations (7) and (22)) can be expressed in terms of the generalized and non-generalized coordinates and time in a vector form as follows:

$$\mathbf{C}\left(\mathbf{q}_r, \mathbf{q}_f, \mathbf{q}_{ch}, \mathbf{s}, t\right) = \mathbf{0} \tag{24}$$

Using the preceding kinematic joint constraint equations that include sliding and wheel/rail contact conditions and the principle of virtual work in dynamics, one can show that the system equations of motion can be written in the following form [22]:

$$\begin{bmatrix} \mathbf{M}_{rr} & \mathbf{M}_{rf} & \mathbf{0} & \mathbf{0} & \mathbf{C}_{\mathbf{q}_r}^{\mathrm{T}} \\ \mathbf{M}_{fr} & \mathbf{M}_{ff} & \mathbf{0} & \mathbf{0} & \mathbf{C}_{\mathbf{q}_f}^{\mathrm{T}} \\ \mathbf{0} & \mathbf{0} & \mathbf{I} & \mathbf{0} & \mathbf{C}_{\mathbf{q}_{ch}}^{\mathrm{T}} \\ \mathbf{0} & \mathbf{0} & \mathbf{0} & \mathbf{0} & \mathbf{C}_{\mathbf{s}}^{\mathrm{T}} \\ \mathbf{C}_{\mathbf{q}_r} & \mathbf{C}_{\mathbf{q}_f} & \mathbf{C}_{\mathbf{q}_{ch}} & \mathbf{C}_{\mathbf{s}} & \mathbf{0} \end{bmatrix} \begin{bmatrix} \ddot{\mathbf{q}}_r \\ \ddot{\mathbf{q}}_f \\ \ddot{\mathbf{q}}_{ch} \\ \ddot{\mathbf{s}} \\ \boldsymbol{\lambda} \end{bmatrix} = \begin{bmatrix} \mathbf{Q}_r \\ \mathbf{Q}_f \\ \mathbf{Q}_{ch} \\ \mathbf{0} \\ \mathbf{Q}_c \end{bmatrix} \tag{25}$$

where subscripts r, f, ch and s refer, respectively, to reference, elastic, Cholesky and non-generalized coordinates; $\mathbf{M}$ is the mass matrix, $\mathbf{C}_{\mathbf{q}}$ is the constraint Jacobian matrix associated with the generalized coordinates, $\mathbf{C}_{\mathbf{s}}$ is the constraint Jacobian matrix associated with the non-generalized coordinates, $\boldsymbol{\lambda}$ is the vector of Lagrange multipliers, $\mathbf{Q}_r$, $\mathbf{Q}_f$ and $\mathbf{Q}_{ch}$ are the generalized force vectors associated with the reference, elastic and Cholesky coordinates, and $\mathbf{Q}_c$ is a quadratic velocity vector that results from the differentiation of the kinematic constraint equations twice with respect to time.

In an alternate approach, one can systematically eliminate the non-generalized coordinates that represent the arc-length and contact surface parameters from the equations of motion. To this end, a set of constraint equations equal to the number of non-generalized coordinates is identified. These constraint equations can be used to write the non-generalized coordinates and their derivatives in terms of the generalized coordinates, velocities and accelerations. This procedure which is explained in details in the literature [7] leads to the following reduced system of equations:

$$\begin{bmatrix} \mathbf{M}_{rr} & \mathbf{M}_{rf} & \mathbf{0} & \mathbf{H}_r^{\mathrm{T}} \\ \mathbf{M}_{fr} & \mathbf{M}_{ff} & \mathbf{0} & \mathbf{H}_f^{\mathrm{T}} \\ \mathbf{0} & \mathbf{0} & \mathbf{I} & \mathbf{H}_{ch}^{\mathrm{T}} \\ \mathbf{H}_r & \mathbf{H}_f & \mathbf{H}_{ch} & \mathbf{0} \end{bmatrix} \begin{bmatrix} \ddot{\mathbf{q}}_r \\ \ddot{\mathbf{q}}_f \\ \ddot{\mathbf{q}}_{ch} \\ \boldsymbol{\lambda}^n \end{bmatrix} = \begin{bmatrix} \mathbf{Q}_r \\ \mathbf{Q}_f \\ \mathbf{Q}_{ch} \\ \mathbf{Q}_{cn} \end{bmatrix} \tag{26}$$

where $\mathbf{H}$, an implicit function of $\mathbf{s}$, is the Jacobian matrix of the constraint equations that is obtained by eliminating the non-generalized coordinates, $\boldsymbol{\lambda}^n$ is the vector of the system Lagrange multipliers that include only independent Lagrange multipliers associated with the sliding joint and wheel/rail contact conditions and other Lagrange multipliers associated with non-contact constraints, and $\mathbf{Q}_{cn}$ is a quadratic velocity vector that results from the differentiation of the constraint equations twice with respect to time. This vector is a function of the surface parameters $\mathbf{s}$ and their first time derivatives. Note that the inertia and generalized forces are not changed as the result of eliminating the non-generalized coordinates.

Equation (25) or (26) can be solved for the accelerations and Lagrange multipliers. Using the accelerations, the independent state equations can be identified and integrated forward in time to determine the coordinates and velocities using multibody system algorithms [18].

6. Pantograph/Catenary Systems

The stability of the pantograph/catenary system is crucial in keeping continuous electric power supply to trains. For this reason, the computer-aided analysis of the pantograph/catenary system is important

to achieve the maximum operating speed of trains. In this section, the components of the catenary cable and pantograph systems used in high-speed trains are briefly discussed.

6.1. Catenary Cable System

Figures 4 and 5 show a catenary system that is used for railroad vehicles. The most common catenary system consists of contact wires and messenger wires, and these wires are connected by droppers that allow only tensile forces. The catenary system also includes supporters, moving brackets, and steady arms (pull-off fittings). The contact wire provides electric power to the pantograph through contact. Repetitive running of the vehicle causes fatigue and wear of the wires and pan-head of the pantograph.

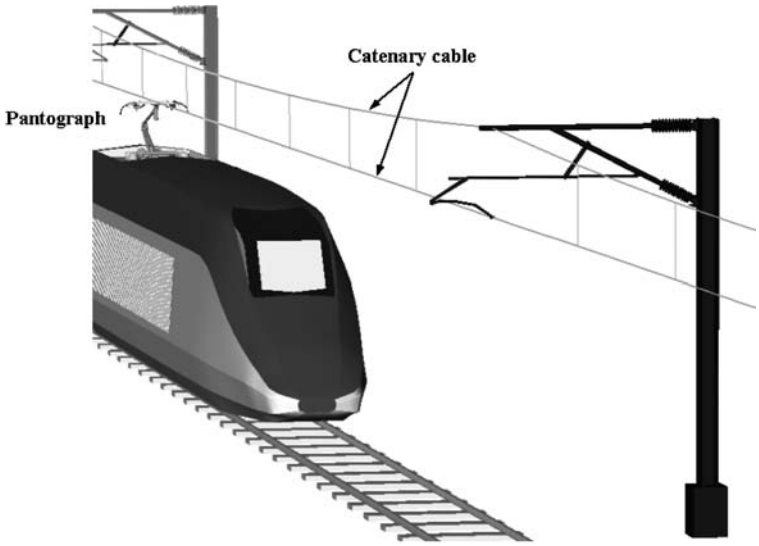

Figure 4. Railroad vehicle with the pantograph/catenary system.

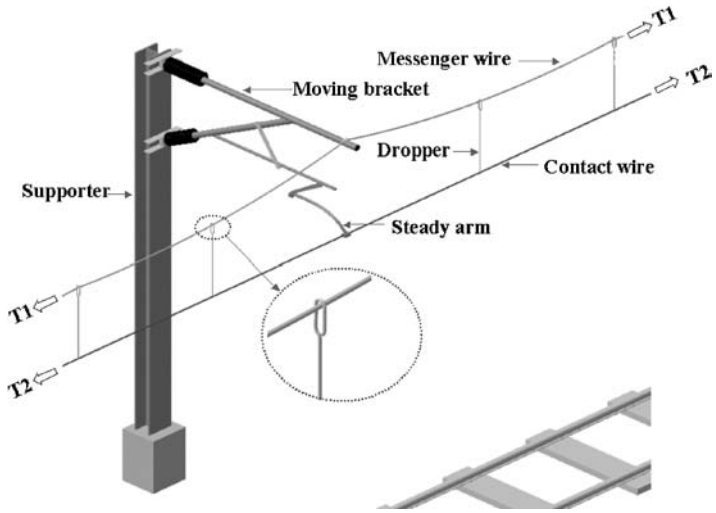

Figure 5. Catenary system.

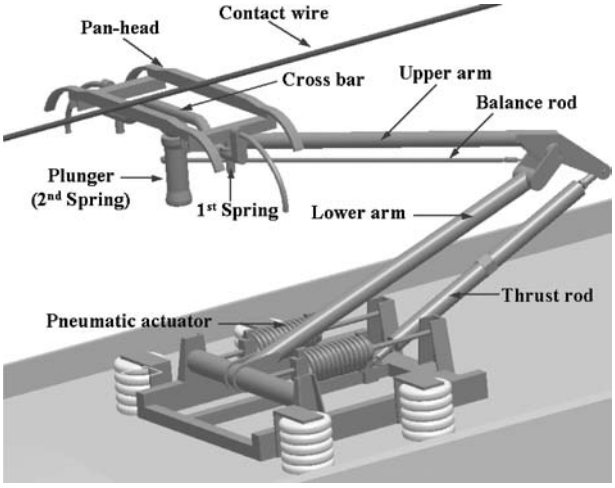

Figure 6. Single arm pantograph.

The messenger wire prevents slanting caused by admissible loading of the contact wire. The messenger and contact wires undergo nonlinear elastic deformations. As shown in Figure 5, the vertical droppers connect the contact and messenger wires, providing additional stiffness and helping in maintaining the system stability. The droppers have high tensile stiffness, but have no resistance to compressions. The horizontal steady arm is used to maintain a shape of the catenary such that wear of the pan-head is reduced. The steady arms are connected to the support using pin joint in order to allow for the contact wire oscillations. The dropper tension between the contact wire and the messenger wire, the span length of the supporter, the gap, the number of droppers, etc. have an effect on the vertical stiffness of the catenary systems.

6.2. PANTOGRAPH SYSTEM

The pantograph is used to draw power from the catenary system during the railroad vehicle operation as shown in Figure 6. The mechanical/electrical interface with the contact wire has an important effect on the stability of the vehicle system. The pantograph in general is subjected to external forces that include aerodynamic forces, static uplift forces, and friction forces caused by the contact. The pantograph model used in the numerical investigation presented in this paper is assumed to consist of four rigid bodies; the pan-head, the plunger, the upper arm and the lower arm. The pan-head, as shown in Figure 7, is connected to the plunger by a spring-damper element. The plunger is connected to the upper arm by a revolute joint, and the upper and lower arms are connected by a revolute joint as well. The lower arm is connected to the car body by a revolute joint.

7. Numerical Example

Figure 7 shows a planar view of the three-dimensional catenary system model used in the numerical investigation presented in this section. The dropper is modeled as a spring with nonlinear characteristics. The dropper is assumed to produce tensile force and zero compressive force. The contact wire which is assumed to be initially straight is discretized using eight beam elements developed using the absolute

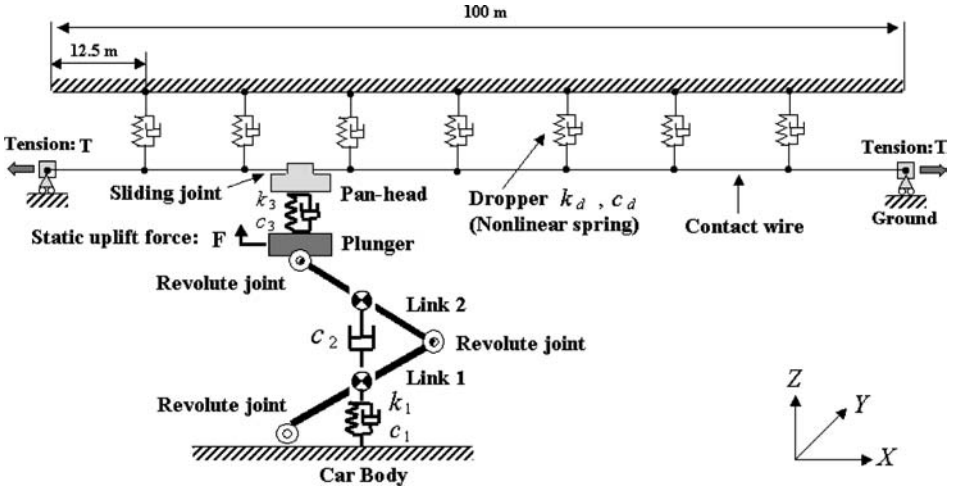

Figure 7. Pantograph/catenary model.

nodal coordinate formulation. For simplicity, the messenger wire is not included in the model examined in this investigation. The density, the cross-section area, and Young's modulus of the contact wire are assumed to be $\rho = 4200.0\,\text{kg/m}^3$, $A = 9.0\,\text{mm}^2$, and $E = 9.0\text{E}{+}10\ \text{N/m}^2$, respectively, while an initial static tension force of $T = 5.0\text{E}{+}3\,\text{N}$ is applied to both ends of the wire. The stiffness and damping coefficients of the dropper are, respectively, assumed to be 2.0E+5 N/m and 1.0E+2 Ns/m. Figure 7 also shows a model of the single arm type pantograph used in this investigation. In this pantograph model, the lower arm is connected to the vehicle body and the upper arm by revolute joints. The mass of the lower and upper arms are both assumed to be 8.0 kg, while the mass of the pan-head and the plunger are, respectively, assumed to be 2.0 and 4.0 kg. The primary spring suspension is attached between the pan-head and the cross bar to absorb high-frequency vibrations arising from the pantograph/catenary interactions, whereas the effect of the secondary spring suspension used to absorb low-frequency vibrations between the cross bar and the plunger is neglected in this investigation. Since a constant static uplift force is applied to the plunger by a pneumatic actuator in order for the pantograph to maintain continuous contact with the contact wire, a static uplift force is always applied to the plunger as shown in Figure 7. The spring constants and damping coefficients used in the pantograph model presented in this section are summarized in Table 1.

Figure 8 shows the detailed three-dimensional vehicle model that includes the pantograph/catenary system, wheel/rail contact, and the bogie suspensions shown schematically in Figure 9. The vehicle consists of two bogies and a car body. If the flexibility of the car body is considered, one can use the floating frame of reference formulation to study the car body deformation. Each bogie consists of two wheel sets, two equalizer bars, a frame and a bolster as shown in Figure 9. The front wheel sets of the leading and trailing trucks are assumed to have a constant forward velocity ($V = 17\,\text{m/s}$). The dimensions and inertia properties of this three-dimensional railroad vehicle model are the same

Table 1. Pantograph spring and damping characteristics.

	Element 1	Element 2	Element 3
Spring constant (N/m)	$k_1 = 40\,000$	$k_2 = 0$	$k_3 = 5000$
Damping coefficient (Ns/m)	$c_1 = 100$	$c_2 = 200$	$c_3 = 50$

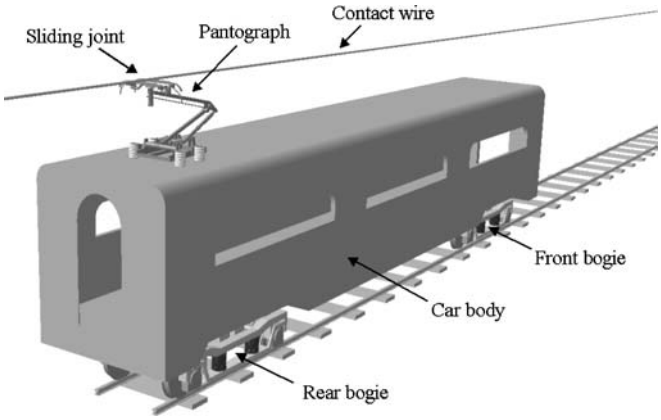

Figure 8. Simulation model of the railroad vehicle.

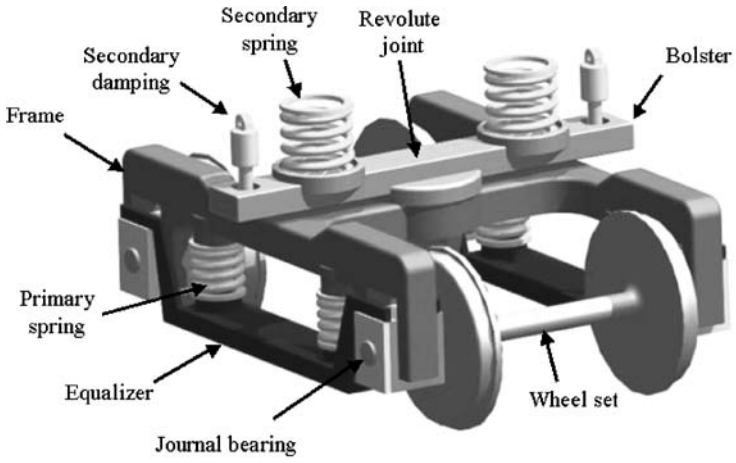

Figure 9. Bogie components.

as previously presented in the literature [6]. Figures 10 and 11 show the vertical displacement and acceleration of the pan-head, while Figure 12 shows the horizontal displacement at the left end of the catenary cable. The high oscillations observed at time $t = 0.0$–2.0 s are attributed to the disturbance due to the fact that the catenary cable was not initially in its static equilibrium configuration. Note that because the pan-head is assumed to always remain in contact with the catenary, the results of Figure 10 can be different if the formulation presented in this paper is modified to account for the loss of contact as described in the following section.

8. Loss of Contact

The loss of contact between the pan-head and the catenary cable is one of the important problems encountered in the operation of high-speed trains. The intermittent contact can lead to loss of continuous power supply and can lead to deterioration in the performance and restriction on the operating speed of the train. For this reason, computer formulations developed for the analysis of the pantograph/catenary

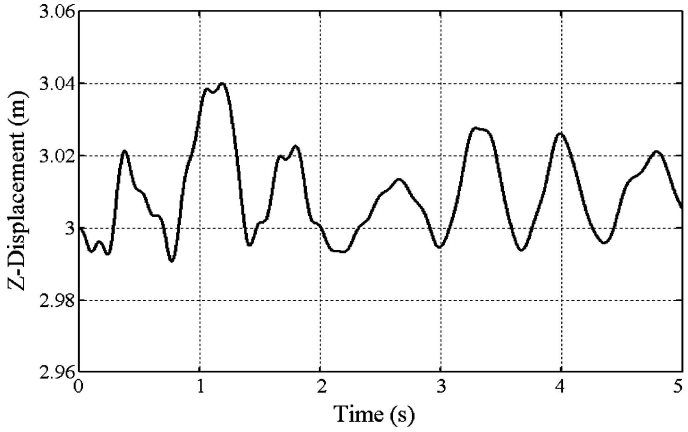

Figure 10. Vertical displacement of the pan-head.

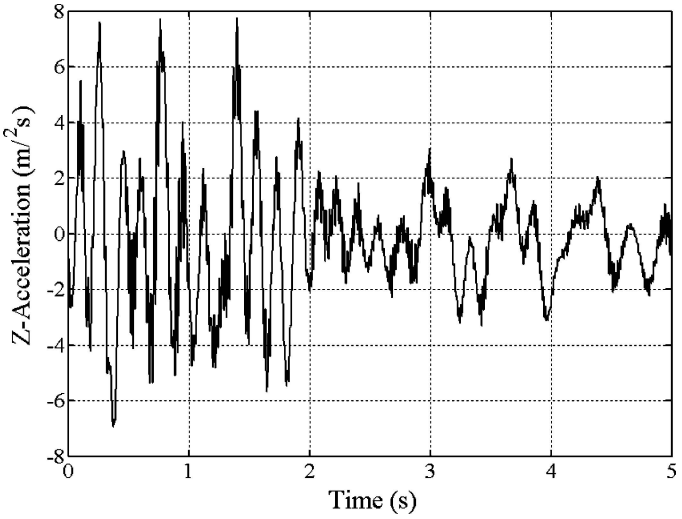

Figure 11. Vertical acceleration of the pan-head.

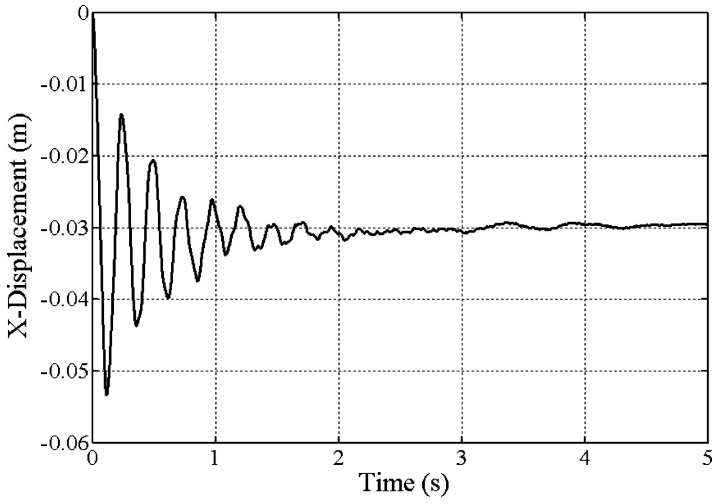

Figure 12. Horizontal displacement at the left end of the contact wire.

system must be capable of addressing the important problem of the loss of contact between the pan-head and the catenary cable.

The formulation presented in this paper can be modified to allow modeling pantograph/catenary systems subject to loss of contact. One approach that can be used to model the loss of contact is to use a force model instead of the sliding joint constraint to represent the contact between the pan-head and the catenary cable. For instance, the first equation in Equation (7) given as $\mathbf{i}_t^{ie} \cdot \mathbf{r}_p^{ij} = 0$ can be used to solve for the arc-length parameter s^{ie} using a procedure similar to the one used in the embedding contact constraint formulation [7]. The other two constraints in Equation (7) can be imposed using a penalty formulation that produces a unilateral force. If the interest is to model the loss of contact in only one direction, the first two constraints of Equation (7) can be imposed as kinematic constraints at the position, velocity and acceleration levels, while the third constraint can be imposed using a penalty method that again produces a unilateral contact force.

9. Summary and Conclusions

In this investigation, a computer formulation for the analysis of the pantograph/catenary interactions in railroad vehicle systems is presented. To model the contact between the pan-head and the catenary cable, a sliding joint formulation that allows for imposing constraints on very flexible catenary cables using the finite element absolute nodal coordinate formulation is presented. This formulation requires the use of non-generalized arc-length coordinates to accurately define the location of the contact point on the cable on line. The dynamic equations of motion for the multibody railroad vehicle system are formulated in terms of the system generalized and non-generalized coordinates. The non-generalized coordinates also include the surface parameters used to describe the contact between the wheel and the rail. An augmented formulation in which the pantograph/catenary sliding joint and the wheel/rail kinematic constraints are adjoined to the differential equations of motion using Lagrange multipliers is presented. Another method that allows for systematically eliminating the non-generalized arc-length parameter is also proposed. In this second method, the equations of motion do not explicitly include the non-generalized accelerations associated with the sliding joint arc-lengths. The use of the formulation presented in this paper is demonstrated using a detailed multibody railroad vehicle model that includes the catenary/pantograph system. This model can be used to study the coupling between the catenary/pantograph system dynamics and the wheel/rail contact forces. Methods for modeling the loss of contact between the pan-head and the catenary cable are also proposed. Active vibration control [23] and comparison between the numerical and experimental data [24] using detailed flexible multibody models are also among the topics that can be addressed in future investigations.

Acknowledgments

This research was supported by Federal Railroad Administration. This support is gratefully acknowledged. The first author would like also to acknowledge the financial support received from the Korea Science and Engineering Foundation.

References

1. Simeon, B., Fuhrer, C., and Rentrop, P., 'Differential algebraic equations in vehicle system dynamics', *Survey on Mathematics in Industry* **1**, 1991, 1–37.

2. Shabana, A. A. and Sany, J. R., 'An augmented formulation for mechanical systems with non-generalized coordinates: Application to rigid body contact problems', *Nonlinear Dynamics* **24**, 2001, 183–204.
3. Kik, W. and Piotrowski, J., 'A fast approximation method to calculate normal load at contact between wheel and rail and creep forces during rolling', in *Proceedings of 2nd Mini Conference on Contact Mechanics and Wear of Rail/Wheel System*, Budapest, 1996.
4. Pombo, J. and Ambrosio, J., 'A wheel/rail contact model for rail guided vehicles dynamics', in *Proceedings of ECCOMAS Thematic Conference on Advances in Computational Multibody Dynamics*, Lisboa, Portugal, 2003.
5. Shabana, A. A., Zaazaa, E. K, Escalona, L. J., and Sany, J. R., 'Development of elastic force model for wheel/rail contact problems', *Journal of Sound and Vibration* **269**, 2004, 295–325.
6. Zaazaa, K., 'Elastic force model for wheel/rail contact in multibody railroad nehicle systems', Ph.D. Dissertation, Department of Mechanical Engineering, University of Illinois at Chicago, Chicago, IL, 2003.
7. Shabana, A. A., Tobaa, M., Sugiyama, H., and Zaazaa, K., 'On the computer formulations of the wheel/rail contact', *Nonlinear Dynamics*, in press.
8. Kalker, J. J., *Three-Dimensional Elastic Bodies in Rolling Contact*, Kluwer, Boston, 1990.
9. Poetsch, G., Evans, J., Meisinger, R., Kortum, W., Baldauf, W., Veitl, A., and Wallaschek, J., 'Pantograph/catenary dynamics and control', *Vehicle System Dynamics* **28**, 1997, 159–195.
10. Manabe, K., 'High-speed contact performance of a catenary-pantograph system', *JSME International Journal* **32**, 1989, 31–40.
11. Yagi, T., Stensson, A., and Hardell, C., 'Simulation and visualisation of the dynamic behaviour of an overhead power system with contact breaking', *Vehicle System Dynamics* **25**, 1996, 31–49.
12. Arnold, M. and Simeon, B., 'Pantograph and catenary dynamics: A benchmark problem and its numerical solution', *Applied Numerical Mathematics* **34**, 2000, 345–362.
13. Wu, T. X. and Brennan, M. J., 'Basic analytical study of pantograph-catenary system dynamics', *Vehicle System Dynamics* **30**, 1998, 443–456.
14. Zhai, W. M. and Cai, C. B., 'Effect of locomotive vibrations on pantograph-catenary system dynamics', *Vehicle System Dynamics* **29**, 1998, 47–58.
15. Lesser, M., Karlsson, L., and Drugge, L., 'An interactive model of a pantograph-catenary system', *Vehicle System Dynamics* **25**, 1996, 397–412.
16. Sugiyama, H., Escalona, J. L., and Shabana, A. A., 'Formulation of three-dimensional joint constraints using the absolute nodal coordinates', *Nonlinear Dynamics* **31**, 2003, 167–195.
17. Sugiyama, H., Mikkola, A. M., and Shabana, A. A., 'A non-incremental nonlinear finite element solution for cable problems', *ASME Journal of Mechanical Design* **125**, 2003, 746–756.
18. Shabana, A. A., *Dynamics of Multibody Systems*, 2nd edn., Cambridge University Press, Cambridge, 1998.
19. Shabana, A. A. and Yakoub, R. Y., 'Three dimensional absolute nodal coordinate formulation for beam elements: Part I and II', *ASME Journal of Mechanical Design* **123**, 2001, 606–621.
20. Park, T.-W., Seo, J.-H., Jung, I.-H., Mok, J.-Y., and Kim, Y.-G., 'Dynamic analysis of a pantograph-catenary cable system for high speed train', in *Proceedings of the Second Asian Conference on Multibody Dynamics*, Seoul, Korea, 2004.
21. Yakoub, R. Y. and Shabana, A. A., 'Use of Cholesky coordinates and the absolute nodal coordinate formulation in the computer simulation of flexible multibody systems', *Nonlinear Dynamics* **20**, 1999, 267–282.
22. Shabana, A. A., 'Non-linear dynamics of multibody systems with generalized and non-generalized coordinates', in *Virtual Nonlinear Multibody Systems*, W. Schiehlen and M. Valasek (eds.), Kluwer Academic Publications, 2003, pp. 1–16.
23. Balestrino, A., Bruno, O., Landi, A., and Sani, L., 'Innovative solutions for overhead catenary-pantograph system: Wire actuated control and observed contact force', *Vehicle System Dynamics* **33**, 2000, 69–89.
24. Collina, A. and Bruni, S., 'Numerical simulation of pantograph-overhead equipment interaction', *Vehicle System Dynamics* **38**, 2002, 261–291.